

---

## Vanishing lead in the Loire River estuary: An example of successful environmental regulation

Briant Nicolas <sup>1,\*</sup>, Knoery Joël <sup>1</sup>, Ferreira Araujo Daniel <sup>1</sup>, Ponzevera Emmanuel <sup>1</sup>,  
Chouvelon Tiphaine <sup>1,3</sup>, Bruzac Sandrine <sup>1</sup>, Sireau Teddy <sup>1</sup>, Thomas Bastien <sup>1</sup>, Mojtahid Meryem <sup>4</sup>,  
Metzger Edouard <sup>4</sup>, Brach-Papa Christophe <sup>2</sup>

<sup>1</sup> Ifremer, CCEM Contamination Chimique des Écosystèmes Marins, F-44000, Nantes, France

<sup>2</sup> Ifremer, LITTORAL, F-83500, La Seyne sur Mer, France

<sup>3</sup> Observatoire Pelagis, UAR 3462, La Rochelle Université - CNRS, F-17000, La Rochelle, France

<sup>4</sup> Université d'Angers, Nantes Université, Le Mans Université, CNRS, Laboratoire de Planétologie et Géosciences, LPG UMR 6112, 49000, Angers, France

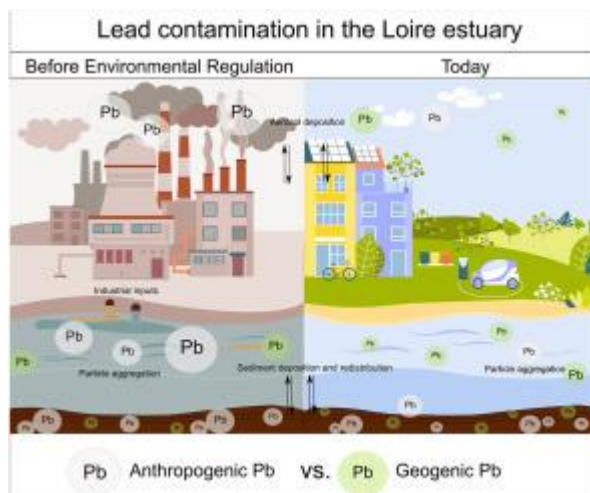
\* Corresponding author : Nicolas Briant, email address : [nicolas.briant@ifremer.fr](mailto:nicolas.briant@ifremer.fr)

---

### Abstract :

The behavior, and history of lead (Pb) contamination in the ecosystem of the Loire estuary was examined using elemental concentrations and Pb isotope data in water, sediment, bivalves, shrimps, and fish. In the estuary and in the surrounding coastal area, Pb concentrations in water and sediment decreased compared to concentrations determined in the 1980s, with concentrations ranging from 15.8 to 65.7 mg kg<sup>-1</sup> in the surface sediment, 0.04–0.26 nM in the water column, and 48.0–77.9 mg kg<sup>-1</sup> in suspended particles. Pb biomonitoring using blue mussels collected by the French Mussel Watch Program over the last 40 years showed a concentration decrease from 3.8 to 0.8 mg kg<sup>-1</sup>. A similar trend is observed in an estuarine sediment core. Changes in accompanying Pb isotope compositions strongly suggest a binary mixing process between Pb derived from terrigenous material and anthropogenic sources. Thus, environmental regulations restricting the release of lead into the environment contribute to a decrease in estuarine levels of this pollutant, which occurs on a decadal time scale.

## Graphical abstract



## Highlights

► Lead isotopes in water and sediment show traces of older lead pollution. ► Dissolved lead concentrations have decreased 100-fold down to background levels. ► Environmental regulations were effective at reducing anthropogenic Pb emissions and load.

**Keywords :** Coastal environment, inorganic element, Pb stable isotopes, Loire estuary

## 38 1. Introduction

39

40 The Loire River basin (117,356 km<sup>2</sup>) is the most important watershed in France and drains  
41 both urbanized and rural areas. It covers a fifth of the French territory but mainly rural areas and  
42 midsize cities. The undammed Loire River has been described as "the last wild river in France"  
43 (Gautier and Grivel 2006). Nevertheless, in its maritime part, the major commercial harbor of Nantes-  
44 St Nazaire has impacted the Loire estuary and its ecosystem functioning (Demaure 1979; Ottmann  
45 1979).

46 Physical and biogeochemical processes occur in estuaries and drive the behavior of various  
47 trace metal elements. Furthermore, estuaries, in the same way as atmospheric transport and others,  
48 contribute to the input of trace metals into the marine environment. The magnitude of metal inputs to  
49 the marine environment depends on their levels in the river waters and on the physicochemical  
50 processes taking place in the estuaries (de Souza Machado et al. 2016). In the middle of the twentieth  
51 century, lead (Pb) was one of the major metal contaminants of the Loire River estuary and is largely  
52 linked to local and regional industrial activities (Elbaz-Poulichet et al. 1984; Boutier et al. 1993;  
53 Couture et al. 2010; Briant et al. 2021). Lead is a non-essential, toxic metal whose biogeochemical  
54 cycle has been affected by human activities to a great degree (Komárek et al. 2008). Lead is regulated

55 by various international and European directives, such as the United Nation Convention on Long-  
56 Range Transboundary Air Pollution (CLRTAP), the European Union (EU) Water Framework  
57 Directive (2000/60/EC), the EU Drinking Water Directive (98/83/EC), or the EU Sewage Sludge  
58 Directive (86/278/EEC). Even if the anthropogenic release of Pb into the environment has been  
59 reduced since the 1980s due to industrial plant closings and gasoline additive bans, the Loire estuary  
60 sediment contamination was still high in 2002 with  $250 \text{ mg kg}^{-1}$  in the lower part of the estuary  
61 (Négreil and Petelet-Giraud 2012). It represents a concentration around five times higher than the  
62 natural background (Négreil and Petelet-Giraud 2012). High Pb sediment concentrations entail  
63 potential remobilization of anthropogenic Pb under its labile forms and/or diffusion into the water  
64 column after particle resuspension (Luoma and Davis 1983; Saulnier and Mucci 2000; Briant et al.  
65 2016). Nowadays, atmospheric aerosols are the dominant source of Pb in the coastal marine  
66 environment and the open ocean (Chen et al. 2016). In terms of stock legacy, Pb inventories inherited  
67 from past emissions could still be progressively released and recycled through the estuarine system  
68 as “new” lead. In the various compartments of an estuary, environmental matrices, like indigenous  
69 bivalves or sediments, act as recording devices that reflect contamination. Among these matrices,  
70 bivalves (e.g., oysters or mussels) from the Loire estuary have been used for four decades as a  
71 biomonitoring device (Claisse 1989). Indeed, they are sessile and bioaccumulate metallic  
72 contaminants, allowing us to evaluate the time-integrated bioavailable Pb (Goldberg 1975; Casas et  
73 al. 2008).

74 In addition to simple environmental lead levels, stable Pb isotopic composition represents a  
75 powerful tool to discriminate between the different sources of environmental Pb (natural, industrial,  
76 leaded gasoline, etc.) (Shotyk et al. 1998; Komárek et al. 2008; Monna et al. 2000). The isotopic  
77 composition of Pb in an environmental matrix, such as bivalves’ soft tissue, corresponds to the  
78 balance between these sources, and source apportionment can be quantified given the different Pb  
79 isotopic signatures (Komárek et al. 2008). It can also be used to understand the estuarine behavior

80 and discriminate between the sources of Pb in the various matrices of the past (e.g., Cariou et al.  
81 2017).

82 Despite all of the geochemical tools available, questions about the behavior of Pb in estuaries  
83 still arise, particularly with regard to the evolution of environmental Pb concentrations according to  
84 health regulations. Is there a latency of estuarine systems or are we witnessing ecosystem resilience?

85 In this study, we report recent Pb levels and isotopic signatures in various environmental  
86 compartments of the Loire estuary ecosystem, including water, suspended particles, sediments, and  
87 endemic organisms, and compare them to previous studies. The aims of the current study are: i) to  
88 better understand the biogeochemical dynamics of Pb in the current Loire estuary system after its  
89 massive, past contamination and ii) to evaluate the actual concentrations in various estuarine  
90 compartments (water, biota, sediments, etc.). The study, in comparison with previous data, makes it  
91 possible to understand the current distribution of Pb in the Loire estuary and to evaluate the impact  
92 of environmental regulations implemented in recent decades.

## 94 **2. Materials and methods**

### 95 **2.1. Water and suspended particles**

96 Water samples were collected during “CAMELIA” sampling campaigns (DOI: 10.18142/281)  
97 in September 2012, April 2013, and February 2014 (Fig. 1). The sampling was conducted along the  
98 salinity gradient from Nantes to the estuarine mouth aboard the R/V *Thalia* during contrasting  
99 freshwater discharge conditions. The Loire freshwater discharge ( $Q_{\text{Loire River}}$ ) was  $\sim 210 \text{ m}^3 \text{ s}^{-1}$ ,  $\sim 1673$   
100  $\text{m}^3 \text{ s}^{-1}$ , and  $\sim 2790 \text{ m}^3 \text{ s}^{-1}$  during the 2012, 2013, and 2014 cruises, respectively (Briant et al. 2021).  
101 The average discharge of the Loire River over the period of 2012–2014 was  $\sim 940 \text{ m}^3 \text{ s}^{-1}$  (Banque  
102 HYDRO – « French Ministry of Ecology, Sustainable Development and Energy »).

103 An all-Teflon pumping system, consisting of 15 mm inner diameter, PFA tubing connected  
104 to a pneumatically-driven PTFE pump (ASTI, France), was used to continuously bring the water into  
105 the ship’s clean, positive pressure laboratory, where all of the sample processing took place. One end

of the Teflon tubing was kept 1 m below the water surface and 5 m off the side of the ship. The other end dispensed water whose conductivity was continuously monitored. At the chosen salinity, water was collected into 2 L PFA bottles held under a laminar air-flow hood. Subsamples were filtered in the clean-room container using N<sub>2</sub> overpressure within 1 h of sampling. Filtered water samples were stored in acid-cleaned HDPE bottles and acidified with 0.1% v/v concentrated nitric acid (Suprapur, Merck®) for dissolved Pb analysis (Pb<sub>d</sub>). Polycarbonate filters (0.45 µm, Nuclepore®) used were previously acid-cleaned, Milli-Q rinsed and, pre-weighed. After filtration, the filters were rinsed with Milli-Q water and stored flat in acid-cleaned polystyrene Petri dishes for suspended particulate Pb analysis (Pb<sub>p</sub>). At the laboratory, the filters were dried and weighed.

Dissolved Pb (Pb<sub>d</sub>) concentrations were determined by Q-ICP-MS (iCAPQ Thermo®) analysis in KED mode (He). Prior to analysis, trace element samples were pre-concentrated using the APDC-DDDC/Freon method (Danielsson et al. 1982). The limit of detection (LOD) was  $6.4 \pm 1.5$  pM (2% ultrapure HNO<sub>3</sub> blank analyses, n = 17), and the quality of the protocol was qualified to the certified reference materials CASS-5 (CRM NRC®, n = 17) (Table SF1).

Suspended particulate Pb (Pb<sub>p</sub>) was determined using the same instrument and protocol as for sediment samples (see section 2.2), except for the sieving step. Particulate organic carbon was measured with a CHN analyzer (Carlo Erba®, Model 1106).

## **2.2. Pb in sediment and biological tissue (mussel, shrimp and fish)**

Seventeen surface sediment sites along the Loire estuary and in Bourgneuf Bay were considered for this study (Fig. 1). The surface sediments were acquired using an Ekman grab in 2014 through the “Réseau d’Observation de la Contamination Chimique” (ROCCh, French Mussel Watch program). After collection, the top of the surface sediment (1–2 cm) samples were collected using a plastic spatula, then frozen in plastic bags, freeze-dried, homogenized, and sieved at <2 mm.

A sediment core “PV1” (~500 cm length) was sampled on the intertidal mudflat “Les Brillantes”, located in the inner Loire estuary near Paimboeuf city (Fig. 1), during the Paleovase

131 mission in March 2015 conducted by the Universities of Angers and Caen (France). A full description  
132 is made in Araújo et al. (2019). Briefly, the core was sub-sampled into 2 cm-thick sediment slices  
133 every 5 cm in the upper meter and every 10 cm for the rest of the sediment core, and the sedimentation  
134 rate was determined. After collection, sub-samples of core PV1 followed the same sample preparation  
135 procedure as the surface sediments.

136 About 200 mg aliquots of dry sediments were digested on a hot plate with 250  $\mu\text{L}$  of  $\text{HNO}_3$ ,  
137 750  $\mu\text{L}$  of  $\text{HCl}$ , and 6 mL of  $\text{HF}$  and heated at 130  $^\circ\text{C}$  for four hours before being brought to dryness  
138 at 100  $^\circ\text{C}$ . A second, 6-hour digestion-step with 4 mL of  $\text{HNO}_3$  and 20 mL of high purity water was  
139 done at 130  $^\circ\text{C}$ . Then, acid digests were transferred to Falcon® tubes and brought to a final volume  
140 of 50 mL with high purity water. Samples were split for subsequent elemental and isotope analyses.  
141 Procedural blanks and a certified reference material (MESS-3 from NRC – CNR®) were processed  
142 along with the samples (Table SF1). The detection limit for the sediment protocol was  $9.5 \pm 1.9 \mu\text{g}$   
143  $\text{kg}^{-1}$  ( $n = 6$ ).

144 Mussels (*Mytilus edulis*) were collected each winter (February–March) at the “Pointe  
145 Chemoulin” site (Fig. 1). The identical sampling protocol has consistently been used since 1979  
146 within the framework of the ROCCh monitoring program. Mussel samples were composed of a pool  
147 of fifty individuals (35–65 mm in shell length, representing 2–3 years of growth). After collection,  
148 bivalves were cleaned of epibiota and depurated for 24 h. Then, soft tissues were thawed,  
149 homogenized with a stainless steel-bladed blender, frozen ( $-20 \text{ }^\circ\text{C}$ ), and finally freeze-dried in acid-  
150 cleaned glass jars. The protocol is fully described in Claisse (1989). Samples (dried and homogenized  
151 powders) were stored in a dark and moisture-regulated room until chemical analysis. Aliquots of ~200  
152 mg of homogenized, freeze-dried bivalves’ soft tissues were digested with 4 mL  $\text{HCl}$  (34%–37%  
153 Suprapur®, SCP Science) and 2.8 mL  $\text{HNO}_3$  (67%–69% Suprapur®, SCP Science) in a microwave  
154 oven (ETHOS UP, Milestone Srl®). Digestates were brought to a final volume of 25 mL with Milli-  
155 Q water (Daskalakis, 1996; USEPA Method 6020A).

156 European sea bass (*Dicentrarchus labrax*) juveniles (fishes of 7–21 cm total length, n = 16) and  
157 their major prey (common shrimps *Crangon crangon*) were collected in spring 2014 in the Loire  
158 estuary between St. Nazaire and Paimboeuf cities (Fig. 1). Back at the laboratory, dead fishes were  
159 dissected and measured. Livers (as the major organ for metal bioaccumulation in fish; e.g., Chouvelon  
160 et al. 2019 and Metian et al. 2013) were collected and stored at -20 °C in acid-cleaned glass vials. For  
161 smaller individuals, livers were pooled, while livers were treated individually for larger fishes. Whole  
162 shrimps were well-rinsed with ultra-pure water before being pooled according to their size (n = 4  
163 pools in total, each composed of 50–200 similar sized individuals) and homogenized using a grinder  
164 with stainless-steel blades. Shrimp and fish liver samples were then freeze-dried and manually  
165 homogenized again, if necessary. For total Pb determination using ICP-MS (iCAP Q Thermo®),  
166 aliquots of ~200 mg (dry weight) of mussel, shrimp, and fish tissues were digested with 3.5 mL of  
167 HCl (34%–37% Suprapur®, SCP Science) and 5 mL of HNO<sub>3</sub> (67%–69% Suprapur®, SCP Science)  
168 in a microwave oven (MARS 5®, CEM). Digests were brought to a final 50 mL volume with Milli-  
169 Q water before analysis. Three different certified reference materials (n = 9), SRM-2976 (mussel  
170 tissue, NIST), DORM-4 (fish protein, NRCC), and DOLT-5 (dogfish liver, NRCC), were analyzed  
171 with the samples, and recovery was within the range of certified values (Table SF1). The detection  
172 limit for the biota analysis was  $3.6 \pm 0.8 \mu\text{g kg}^{-1}$  (n = 12). Before Pb isotope analysis, digests of  
173 shrimp and fish tissues were concentrated again by evaporation on a heat block and recovery in 5 mL  
174 of 3% HNO<sub>3</sub>.

### 175 2.3. Stable Pb Isotope Analysis

176 Stable Pb isotopes were determined on prepared samples of dissolved and suspended  
177 particulate Pb samples from the CAMELIA summer 2012 campaign, on core PV1 and ROCCh  
178 sediment samples, on estuarine fishes and shrimps, and on ROCCh mussel samples from 1981 and  
179 2018. The stable Pb isotope ratios were determined by ICP-MS (iCAP Q Thermo®). The relative  
180 ratios among three stable isotopes (<sup>206</sup>Pb, <sup>207</sup>Pb, and <sup>208</sup>Pb) are reported. Signal intensity was recorded



100 times over  $1.2 \times 10^{-2}$  s for  $^{206}\text{Pb}$  and  $^{207}\text{Pb}$  and  $1.0 \times 10^{-2}$  s for  $^{208}\text{Pb}$ . This procedure was repeated five times for each sample. Mass bias and instrumental drift was corrected with a standard bracketing method by analyzing the certified reference material SRM-981 from NIST after each sample (Araújo et al. 2019). The internal precision of the instrument, expressed as relative standard deviation ( $n = 46$ ), was 0.11% and 0.16% for the  $^{206}\text{Pb}/^{207}\text{Pb}$  ( $1.0933 \pm 0.0012$ , 1SD) and  $^{206}\text{Pb}/^{208}\text{Pb}$  ( $0.4612 \pm 0.0007$ , 1SD) ratios, respectively. Since reproducibility and precision of Q-ICP-MS analyses can be lower than thermal ionization (TIMS) or multi-collector plasma mass spectrometry (MC-ICP-MS) (Gulson et al. 2018), some samples were re-mineralized and reanalyzed in order to verify the associated errors and repeatability of measurements. Reanalysis of sediment ( $n = 3$ ) and bivalve ( $n = 8$ ) samples showed an external relative standard deviation of 0.11% and 0.31% in sediment and 0.28% and 0.44% in bivalves for the  $^{206}\text{Pb}/^{207}\text{Pb}$  and  $^{206}\text{Pb}/^{208}\text{Pb}$  ratios, respectively.

#### 2.4. Loire river fluxes

For each sampling cruise, fluxes of  $\text{Pb}_d$  (Eq. 1) and  $\text{Pb}_p$  (Eq. 2) were calculated by combining mean river discharges during the cruises with measured  $\text{Pb}_d$ ,  $\text{Pb}_p$ , and suspended particulate matter (SPM) concentrations.

$$F_{\text{Pbd}} = Q' (\sum_i^n (Q_i \cdot \text{Pb}_d) / \sum_i^n Q_i) \quad (1)$$

$$F_{\text{Pbp}} = Q' (\sum_i^n (F_{\text{SPMi}} \cdot \text{Pb}_p) / \sum_i^n Q_i) \quad \text{with} \quad F_{\text{SPMi}} = \text{SPM}_i \cdot Q_i \quad (2)$$

where  $F_{\text{Pbd}}$  and  $F_{\text{Pbp}}$  are the dissolved and particulate discharge-weighted daily fluxes ( $\text{kg d}^{-1}$ ), respectively,  $Q_i$  was the daily average water discharge ( $\text{m}^3 \text{d}^{-1}$ ) of the sampled day ( $i$ ),  $Q'$  ( $\text{m}^3 \text{d}^{-1}$ ) was the campaign water discharge (mean of  $Q_i$  during campaign), and  $F_{\text{SPMi}}$  was the daily suspended particulate matter ( $\text{SPM}_i$ ) flux ( $\text{kg d}^{-1}$ ). This approach was also used in Briant et al. (2021) for other metals and followed the Boyle et al. (1974) model, appropriate for the salt-wedge linear Loire estuary. However, with all other parameters being equal, it is biased in case of time-varying water-flow before and during the sampling campaign.

## 205 2.5. Statistics

206 All descriptive and multivariate statistics were performed using R software version 4.1.1 and  
207 the “RcmdrMisc”, “dplyr”, and “ggplot2” packages.

## 209 3. Results

### 210 3.1 Dissolved and particulate Pb concentrations and isotope ratios in the Loire estuary

211 Dissolved and particulate Pb samples from estuarine waters were collected during three  
212 contrasted Loire discharge conditions (Briant et al. 2021) observed in 2012–2014. Average  $Pb_d$  and  
213  $Pb_p$  concentrations ( $0.15 \pm 0.07$  nM and  $62.9 \pm 6.6$  mg kg<sup>-1</sup>, respectively) were quite similar for the  
214 three cruises, with concentrations ranging from 0.04 to 0.26 nM for  $Pb_d$  and from 48.0 to 77.9 mg kg-  
215 <sup>1</sup> for  $Pb_p$  (Table I). From slightly higher riverine end-member levels, dissolved Pb concentrations  
216 decreased along the increasing salinity gradient following a straight theoretical dilution line and were  
217 slightly impacted by the varying river flow conditions (Table I). During summer 2012, at low flow  
218 conditions ( $\sim 210$  m<sup>3</sup> s<sup>-1</sup>), the average  $Pb_d$  concentration was  $0.16 \pm 0.04$  nM, while the average  $Pb_d$   
219 concentration was  $0.12 \pm 0.05$  nM during winter 2014 with high river flow conditions ( $\sim 2790$  m<sup>3</sup> s<sup>-</sup>  
220 <sup>1</sup>). Even lower  $Pb_d$  concentrations were determined during spring 2013 under intermediate river flow  
221 conditions ( $1,673$  m<sup>3</sup> s<sup>-1</sup>) with an average  $Pb_d$  concentration of  $0.08 \pm 0.03$  nM. The dissolved Pb  
222 concentrations measured in the Loire estuary were in the range of concentrations reported by Waeles  
223 et al. (2008) and almost ten times lower than earlier studies in the Loire by Boutier et al. (1993) or in  
224 the Seine River (Chiffolleau et al. 1994) (Fig. 2). Both dissolved and particulate Pb in the Loire  
225 estuary, reported in this study, were in the range of world river average concentrations (e.g., Viers et  
226 al. 2009; Table SF2).

227 Pb isotope ratios from dissolved and particulate samples of the summer 2012 cruise are reported in  
228 Table I. For  $Pb_d$ ,  $^{206}Pb/^{207}Pb$  ratios ranged from 1.157 to 1.180, and  $^{206}Pb/^{208}Pb$  ratios ranged from

0.474 to 0.480. Concerning  $Pb_p$ ,  $^{206}Pb/^{207}Pb$  ratios ranged from 1.170 to 1.182, and  $^{206}Pb/^{208}Pb$  ratios ranged from 0.478 to 0.481.

### 3.2. Lead concentrations and isotope ratios in sediment and biological tissue

Surface sediments from the Loire estuary and nearby coastal sites sampled in 2014 ranged from 15.8 to 65.7 mg kg<sup>-1</sup>. The highest concentrations were observed near the river mouth and close to Nantes city (64 ± 1 mg kg<sup>-1</sup>). The lowest concentrations were observed at the coastal sites with values around 25 ± 9 mg kg<sup>-1</sup>. Al-normalized data ranged from 2.3 to 11.9 (Table II), and enrichment factors (EF) were less than 1.1, which indicates a negligible anthropogenic contamination compared to the local geochemical background, as determined using concentrations in the lowest part (>200 cm) of the PV1 core. Sediment lead isotope ratios ranged from 1.158 to 1.187 for  $^{206}Pb/^{207}Pb$  ratios and from 0.473 to 0.480 for  $^{206}Pb/^{208}Pb$  ratios (Fig. 3A). The lowest  $^{206}Pb/^{207}Pb$  ratio (1.158) was at the “Paimboeuf” site, which is routinely in the turbidity maximum zone (TMZ) and, unsurprisingly, adjacent to a former leaded gasoline additive plant. Lower  $^{206}Pb/^{207}Pb$  and  $^{206}Pb/^{208}Pb$  ratios could be explained by the presence and/or remobilization of legacy anthropogenic Pb with lighter isotopic composition. The highest  $^{206}Pb/^{207}Pb$  values (~1.187) were localized outside the estuary at the southern coastal studied sites “Mariolle HF3” and “Embarcadère” (see map in Fig. 1). Except for a relative “hotspot” near Paimboeuf, no geographical trend could be observed from the distribution of Pb isotope ratios in the sediment of the Loire estuary, suggesting laterally homogeneous mixing of surficial sediments. Most of the Pb isotope ratios in surface sediment samples were in the range of those of SPM, all being closer to the “natural background” ratios found at 200 cm depth in the PV1 core. Those found by Négrel and Petelet-Giraud (2012), which were collected in 1997, had more elevated estuarine  $^{206}Pb/^{207}Pb$  values (between 1.145 to 1.151), possibly due to the greater proximity of the plant’s activity period.

The lead concentration depth profile of the PV1 core displays a general increase from the ~96 cm deep horizon (76 mg kg<sup>-1</sup>), followed by a peak at ~14 cm (134 mg kg<sup>-1</sup>) then a sharp decline from

14 cm deep to the top of the core (Table II). Lead isotope ratios ranged from 1.142 to 1.184 for  $^{206}\text{Pb}/^{207}\text{Pb}$  ratios and from 0.472 to 0.479 for  $^{206}\text{Pb}/^{208}\text{Pb}$  ratios. The general trend observed in Pb concentrations is also observed in isotope ratios. The deepest part of the sediment core presents the highest Pb isotope ratios while the peak of concentration, around 14 cm depth, presents the lowest isotope ratios ( $1.142$   $^{206}\text{Pb}/^{207}\text{Pb}$  and  $0.472$   $^{206}\text{Pb}/^{208}\text{Pb}$ ).

Pb isotope ratios measured in seabass livers (mean  $\pm$  SD for  $^{206}\text{Pb}/^{207}\text{Pb} = 1.169 \pm 0.003$  and  $^{206}\text{Pb}/^{208}\text{Pb} = 0.477 \pm 0.001$ ) and in their typical prey (whole shrimps) ( $^{206}\text{Pb}/^{207}\text{Pb} = 1.172 \pm 0.007$ ;  $^{206}\text{Pb}/^{208}\text{Pb} = 0.477 \pm 0.002$ ) were similar (Fig. 3B), showing Pb does transfer unfractionated through trophic levels in the Loire estuary. Hence, the Pb isotope ratio results from seabass and shrimps do integrate the Pb distribution in the food web of the Loire estuary system in 2014. Pb isotope ratios measured in these biological samples were also in the range of those measured in surface sediment from 2014 and in dissolved samples from the Loire estuary, strongly suggesting a similar origin of lead (Figs. 3A and 3B). More specifically, fish and shrimp isotopic Pb signatures suggest that Pb sources currently integrating the Loire food web are a mixture of legacy industrial emissions and natural Pb sources (see discussion 4.2). This is consistent with other recent studies using Pb isotope ratios in fish from other coastal regions of the world showing that bioaccumulated coastal Pb originates from both anthropogenic (atmospheric aerosols, fossil fuels...) and natural geogenic sources, with anthropogenic sources even surpassing the natural ones in marine fish (Li et al. 2020; Chételat et al. 2022).

## 4. Discussion

### 4.1 Behavior of Pb in Loire estuary

Since Pb concentrations in Loire River waters are low, the present distributions of  $\text{Pb}_d$  through the salinity gradient are monotonous and near the biogeochemical background. It contrasts with previous observations when estuarine Pb levels were markedly higher. During the 1980s and late 1990s,  $\text{Pb}_d$  concentrations showed an increase of concentrations in the 1–17 salinity range (Boutier

279 et al. 1993; Fig. 2). The contribution of industrial inputs in the estuarine waters was identified as the  
280 main  $Pb_d$  origins. Then, the Octel corporation was producing tetra-alkyl lead ( $\sim 20,000 \text{ T y}^{-1}$ ) between  
281 1938 and 1996 and discharged about  $50 \text{ kg d}^{-1}$  into the estuary during this period (Anonymous 1993).  
282 Later, Waeles et al. (2008) observed a non-conservative behavior regarding a theoretical dilution line,  
283 which suggested a removal of the dissolved metal. This pattern has been observed in many estuaries  
284 (Windom and Niencheski 2003) linked to metal adsorption to suspended particles or coprecipitation  
285 with iron and manganese oxides (Elbaz-Poulichet et al. 1984; Négre and Petelet-Giraud 2012).

286  $Pb$  concentrations in particulate matter were even more stable regardless of riverine discharge  
287 conditions and the SPM concentrations, with an average  $Pb_p$  concentration of  $62.3 \pm 7.4 \text{ mg kg}^{-1}$ . The  
288 range of  $Pb_p$  concentration was between 48.0 and  $77.9 \text{ mg kg}^{-1}$ . These variations of concentrations in  
289 SPM and the important differences of concentrations between dissolved and particulate  $Pb$  are  
290 reflected by the particle-water distribution coefficient ( $\log_{10} K_D$ , Sung 1995), which is high and quite  
291 constant during both the temporal surveys and the estuarine transects (6.1 to  $6.8 \text{ L kg}^{-1}$ ). The particle-  
292 water distribution coefficient, expressed as  $\log_{10} K_D$  ( $\text{L kg}^{-1}$ ) (Sung 1995), describes the metal  
293 partitioning between particulate and dissolved concentrations. Briefly,  $\log_{10} K_d$  (in  $\text{L kg}^{-1}$ ) is the ratio  
294 between  $Pb_p$  ( $\text{mg kg}^{-1}$ ) and  $Pb_d$  ( $\text{mg L}^{-1}$ ).  $Pb$  reactivity and affinity for particles is important  
295 (Brügmann et al. 1985; Balls 1989). The conservative behavior of  $Pb_d$  observed in 2013 could be  
296 related to particle concentrations through the estuary, which leads to stable dissolved and particulate  
297  $Pb$  distributions, even if the estuarine conditions are changing. The estuary thus appears as a  
298 transitional environment that does not retain nor release significant  $Pb_d$ . It seems that the  $Pb$   
299 concentrations in the estuarine waters have reached an equilibrium with available particles and they  
300 follow a simple dilution behavior between upstream stations and the river mouth (Fig. 2).

301 Riverine influxes and effluxes have been calculated assuming equations reported in the  
302 companion paper (Briant et al. 2021) and following the Boyle et al. (1974) model. River fluxes of  
303 elements are strongly influenced by varying discharges throughout the year, so only the most

304 contrasted discharge conditions of the river are presented here to illustrate the wide range of variation  
305 of hydrological conditions and subsequent changes in Pb inputs and effluxes of the Loire River.  
306 During summer 2012, when a low river discharge ( $Q \sim 210 \text{ m}^3 \text{ s}^{-1}$ ) was recorded, the calculated  
307 riverine  $\text{Pb}_d$  input flux was  $0.35 \pm 0.02 \text{ kg d}^{-1}$  and the  $\text{Pb}_p$  flux was  $11.9 \pm 0.6 \text{ kg d}^{-1}$ . During winter  
308 2014, the Loire River discharge was high with  $Q \sim 2,790 \text{ m}^3 \text{ s}^{-1}$ , so the calculated influxes were  $8.0 \pm$   
309  $1.2 \text{ kg d}^{-1}$  for  $\text{Pb}_d$  and  $821.7 \pm 119.0 \text{ kg d}^{-1}$  for  $\text{Pb}_p$ . Despite lower SPM, the latter was much higher  
310 due to the high-water discharge. To look at the potential extreme range of Pb fluxes in the Loire River,  
311 extrapolation fluxes have been calculated using the water discharge of the 2012 and the 2014  
312 campaigns. Extrapolated annual Pb fluxes in the Loire River ranged from  $0.13 \text{ T y}^{-1}$  to  $2.93 \text{ T y}^{-1}$  for  
313  $\text{Pb}_d$  and from  $4.36 \text{ T y}^{-1}$  to  $299.92 \text{ T y}^{-1}$  for  $\text{Pb}_p$ . Dissolved fluxes from the present study were lower  
314 than fluxes calculated by Boutier et al. (1993) and Anonymous (1987; in Boutier et al. 1993) with  
315  $10.95$  and  $18.25 \text{ T y}^{-1}$ , respectively, but in the range of fluxes determined by Waeles et al. (2008).  
316 Calculated fluxes from this study were in the range of the Seine River ( $\text{Pb}_p = 96 \text{ T y}^{-1}$ ; Thévenot et  
317 al. 2009) but one order of magnitude lower than large world rivers, such as the Yellow River ( $\text{Pb}_p =$   
318  $4,049 \text{ T y}^{-1}$ ; Hu et al. 2015). This difference with the large rivers can be explained by the difference  
319 in flow rate (around 2 to 3 times less for the Loire) and suspended matter load (up to 100 times less  
320 for the Loire) and by the Pb inputs associated with anthropogenic activities present in the estuarine  
321 watershed.

322 Current observations show that the estuarine region is neutral with respect to fluxes of Pb and  
323 that an equilibrium has been reached between the different estuarine compartments; however,  
324 knowledge of the fate of buried Pb becomes important for stakeholders and water resource managers.  
325 Indeed, beyond the well-known estuarine biogeochemical behavior of lead, the questions about the  
326 trajectory of the different compartments once the pollution ceases are worthy of investigation.

327 The distribution of Pb isotope ratios in the estuarine water along the estuary was stable, with a  
328 ratio variation around  $1.007 \pm 0.003$ . Paired dissolved and particulate samples have systematically

distinguishable isotope ratios. Particulate Pb is always slightly enriched in  $^{206}\text{Pb}$ , resulting in higher  $^{206}\text{Pb}/^{207}\text{Pb}$  (+0.01) and  $^{206}\text{Pb}/^{208}\text{Pb}$  (+0.001) ratios. The fractionation is constant and small throughout the estuary allowing us, as it is generally assumed for Pb isotopes, to use Pb isotopes as a tracer of pollution (Rabinowitz & Wetherill 1972; Wiederhold 2015). No significant correlations with salinity (Spearman test,  $p$ -values = 0.37) or particulate organic carbon (Spearman test,  $p$ -values = 0.15) were found. Slight variation in dissolved and particulate  $^{206}\text{Pb}/^{207}\text{Pb}$  ratios through the estuary were observed with the variations of SPM concentrations, even if it was not significant (Spearman test,  $p$ -value = 0.88). From the riverine end-member at the “Montjean” site, which is 117 km (PK117) upstream of St Nazaire,  $^{206}\text{Pb}/^{207}\text{Pb}$  ratios were close to “geogenic” values (Komárek et al. 2008) (Table I,  $\text{Pb}_d$ :  $^{206}\text{Pb}/^{207}\text{Pb} = 1.172$  and  $^{206}\text{Pb}/^{208}\text{Pb} = 0.479$ ;  $\text{Pb}_p$ :  $^{206}\text{Pb}/^{207}\text{Pb} = 1.182$  and  $^{206}\text{Pb}/^{208}\text{Pb} = 0.480$ ). Then, in the mixing and tidally active parts of the estuary, where SPM concentrations increase, the  $^{206}\text{Pb}/^{207}\text{Pb}$  ratios decreased. This could be explained by a potential remobilization of a small part of anthropogenic Pb. In 1986, Elbaz-Poulichet et al. found slightly lower  $^{206}\text{Pb}/^{207}\text{Pb}$  ratios for particulate Pb in the Loire estuary, with values ranging from 1.145 to 1.158 and much lower  $^{206}\text{Pb}/^{207}\text{Pb}$  ratios for dissolved Pb with  $1.129 \pm 0.007$ . It was explained by the input of industrial tetra-alkyl Pb in the estuary with a low  $^{206}\text{Pb}/^{207}\text{Pb}$  ratio during the 1980s, which was also observed and suggested by Boutier et al. (1993).

#### **4.2 Evolution of Pb isotopes in the estuary over three decades: a trajectory of ecosystemic resilience**

The results from the sediment core and mussel analyses (Fig. 4) show the general decrease in elemental Pb levels, accompanied with changes of Pb isotopic signatures between the mid-1980s and the present. Such changes indicate source apportionments changes. The concomitant evolution of concentrations and isotope ratios are consistent with a single major source during this period. Then, the decrease of Pb concentrations is due to increasingly stringent limits on Pb emissions into the environment, such as the 1998 Aarhus Protocol on Heavy Metals, as reported by Couture et al. (2010).

354 Using a strategy that involved projecting an isotopic ratio as a function of  $1/[Pb]$  of samples  
355 from the same geographical entity, the isotopic ratio of the contaminating source can be determined  
356 (Supplementary File). This method, which has its drawbacks as well, has often been applied  
357 convincingly (e.g., Ferrand et al. 1999, Alleman et al. 2000, and Cloquet et al. 2006). From those  
358 results, the evolution of the inputs of Pb in the sediment of the Loire estuary can be retraced. Before  
359 the twentieth century (deeper than 96 cm in the PV1 core), the Pb isotope ratio from the source is  
360 located around 1.180 for  $^{206}Pb/^{207}Pb$ . This ratio corresponds to ratios found by Négrel and Petelet-  
361 Giraud (2012) for weathering of the natural geologic rocks. Between 69 cm and 15 cm depth, which  
362 corresponds approximately to the 1920–1995 period, Pb concentrations and isotopic ratios rose. The  
363 estimated Pb isotope ratios for the source (1.077 for  $^{206}Pb/^{207}Pb$ ) are consistent with European  
364 gasoline (Monna et al. 1997) with  $^{206}Pb/^{207}Pb$  ratios in gasoline ranging from 1.061 to 1.094. Finally,  
365 the Pb concentrations decrease in the upper part of the core and the ratios rise. It is estimated that the  
366 current potential source has a  $^{206}Pb/^{207}Pb$  ratio of approximately 1.110. This ratio is still quite low  
367 and corresponds to an industrial footprint (Harlavan, Almogi-Labin, and Herut 2010; Komárek et al.  
368 2008); however, looking at the ratios and the evolution of the Pb concentrations, we can hypothesize  
369 that the Pb found in the top layer of sediment is a mix of old contaminated sediment and new Pb ratios  
370 linked to new atmospheric inputs and geogenic inputs from the watershed.

371 The evolution of Pb concentrations and ratios in mussels at the estuary mouth allows us to  
372 verify this information (Figs. 4A and 4B). Between 1981 and 2008, mussel Pb concentrations  
373 decrease 4- to 5-fold from 3.8 to 0.8 mg kg<sup>-1</sup>. Between 1985 and 1995, ratios as low as 1.120 to 1.140  
374 were reflecting the composition of anthropogenic Pb inputs from various sources [e.g., aerosols  
375 (Bollhöfer and Rosman 2001), automobile exhausts (Monna et al. 1997), and gasoline (Komárek et  
376 al. 2008)]. If airborne particulate matter, incinerator ash, and gasoline have represented the major  
377 sources of Pb pollution in urban areas in France during the 1990s (Monna et al., 1997), the major part  
378 of the Pb contamination in the Loire estuary was linked to the presence of an alkyl Pb plant located



379 in Paimboeuf (Elbaz-Poulichet et al. 1986; Boutier et al. 1993). From 1937 to 1993, the chemical  
380 plant produced tetra ethyl and tetra methyl Pb, which released up to  $23 \times 10^3$  kg  $y^{-1}$  of Pb in the Loire  
381 estuary (Boutier et al. 1993), overwhelming all other sources including geogenic ones (Couture et al.  
382 2010). The increase of  $^{206}\text{Pb}/^{207}\text{Pb}$  ratios between 1985 and 2005 could be linked with the progressive  
383 closure of the plant and the decreased phasing-out of leaded gasoline production (Shiel et al. 2012).  
384 Concomitantly, a relative increase in natural Pb fraction bioaccumulated in the bivalves could be  
385 observed.

386 After 2008, the  $^{206}\text{Pb}/^{207}\text{Pb}$  and  $^{206}\text{Pb}/^{208}\text{Pb}$  ratios stabilized around  $1.167 \pm 0.002$  and  $0.477 \pm$   
387  $0.001$ , respectively, which is consistent with ratios observed in the surface sediments and the signature  
388 of particles originating from bedrock weathering upstream of the estuary (Négreel and Petelet-Giraud  
389 2012). Looking at mussels as organisms representative of their estuarine environment, Pb  
390 concentrations (and hence inputs) in the Loire River seem to approach the geogenic levels.

391 Although each source of Pb has a specific isotopic composition, it is important to know that  
392 the distinct, well-mixed geochemical reservoirs (i.e., sediment, water, atmosphere) are linked by  
393 fluxes of Pb and, therefore, a given isotopic composition within a given reservoir results from the  
394 mixing of the different sources (Komárek et al. 2008). Sediment and organisms (mussels, seabass,  
395 and shrimps) considered in our study exhibit present-day (after 2014)  $^{206}\text{Pb}/^{207}\text{Pb}$  ratios ranging  
396 between 1.161 to 1.187. This narrow range is close to the geochemical background ratio and shows  
397 that the Loire estuary seems to be returning to its natural baseline, both in terms of ratios and  
398 concentrations.

399 Although a currently active source with an industrial isotope signature is possible, remobilization of  
400 legacy Pb likely occurs in the estuary. If this hypothesis is verified, the Pb isotope signature of  
401 estuarine organisms will asymptotically approach values of the geogenic background at a temporal  
402 rate limited by the exhaustion of the legacy industrial Pb buried in the entire estuary.

## 403 **5. Conclusion**

404 Water, sediment, biota, and their elemental concentrations and Pb isotope ratios were used to  
405 examine the behavior of Pb in the Loire estuary. Time-integrated matrices, such as a sediment core  
406 and estuarine dwelling organisms, show a decrease in concentrations since the end of the twentieth  
407 century. The Pb levels in the Loire estuary have returned to near background levels, but anthropic Pb  
408 is still observable. Thus, environmental laws and directives have a key role in reducing harmful metal  
409 emissions, and their effects are observable on a decadal time scale. While this study was conducted  
410 with relatively low precision isotopic measurements, future studies of local Pb sources (atmospheric  
411 deposits, water from urban catchment areas, and wastewater treatment plants) could provide  
412 additional details and help refine our understanding of the origin and fate of Pb in the Loire estuary.  
413 Using new proxies, like rare earth element (REE) patterns or other stable isotopic systems of emergent  
414 metal contaminants (e.g. Li, Sb), could also be used to differentiate past from current anthropic  
415 emissions. Finally, sediment diagenetic processes linked to the tide or climate change scenarios are  
416 also interesting ways of investigating Pb behavior.

## 418 **Acknowledgements**

419

420 This study is part of the RS2E – OSUNA project funded by the Région Pays de la Loire. Sediment  
421 core PV1 was sampled during the Paleovase mission conducted in 2015 by universities of Angers and  
422 Caen (France) and financed by the OSUNA. Thanks to Jean-François Chiffolleau, Jeanne Bretaudeau-  
423 Sanjuan, Emmanuelle Rozuel, Dominique Auger, Sylvette Crochet, the LERMPL team and the N/O  
424 Thalia crew for their help during the CAMELIA series of cruises (DOI: 10.18142/281). We are also  
425 thankful to all participants of the Paleovase mission.

## 426 **Authors contributions**

427

428 **Nicolas Briant:** Data interpretation, Writing- Original draft preparation, Reviewing and Editing. **Joël**  
 429 **Knoery** and **Christophe Brach-Papa:** Conceptualization, Methodology, Supervision, Reviewing,  
 430 Editing. **Sandrine Bruzac, Teddy Sireau** and **Bastien Thomas:** Methodology, Analytics and data  
 431 generation. **Tiphaine Chouvelon, Emmanuel Ponzevera** and **Daniel F. Araujo:** Writing-  
 432 Reviewing. **Edouard Metzger** and **Meryem Mojtahid:** Conceptualization of the cruise, Reviewing.  
 433 All authors commented on the manuscript. All authors read and approved the revised manuscript.

## 434 435 **References** 436

- 437 Alleman, L. Y., B. Hamelin, A. J. Veron, J. C. Miquel, and S. Heussner. 2000. "Lead Sources and  
 438 Transfer in the Coastal Mediterranean: Evidence from Stable Lead Isotopes in Marine  
 439 Particles." *Deep Sea Research Part II: Topical Studies in Oceanography*. 47 (9–11): 2257–79.
- 440 Anonymous. 1993. "Cartographie de La Pollution Industrielle.Principaux Rejets Industriels  
 441 (Résultats 1990)." Paris.
- 442 Araújo, DF, E Ponzevera, N Briant, J Knoery, T Sireau, M Mojtahid, E Metzger, and C Brach-Papa.  
 443 2019. "Assessment of the Metal Contamination Evolution in the Loire Estuary Using Cu and  
 444 Zn Stable Isotopes and Geochemical Data in Sediments." *Marine Pollution Bulletin* 143  
 445 (June): 12–23. <https://doi.org/10.1016/j.marpolbul.2019.04.034>.
- 446 Balls, P. W. 1989. "The Partition of Trace Metals between Dissolved and Particulate Phases in  
 447 European Coastal Waters: A Compilation of Field Data and Comparison with Laboratory  
 448 Studies." *Netherlands Journal of Sea Research* 23 (1): 7–14. [https://doi.org/10.1016/0077-7579\(89\)90037-9](https://doi.org/10.1016/0077-7579(89)90037-9).
- 450 Bollhöfer, A, and KJR Rosman. 2001. "Isotopic Source Signatures for Atmospheric Lead: The  
 451 Northern Hemisphere." *Geochimica et Cosmochimica Acta* 65 (11): 1727–40.  
 452 [https://doi.org/10.1016/S0016-7037\(00\)00630-X](https://doi.org/10.1016/S0016-7037(00)00630-X).
- 453 Boutier, B, JF Chiffoleau, D Auger, and I Truquet. 1993. "Influence of the Loire River on  
 454 Dissolved Lead and Cadmium Concentrations in Coastal Waters of Brittany." *Estuarine,  
 455 Coastal and Shelf Science* 36 (2): 133–45. <https://doi.org/10.1006/ecss.1993.1009>.
- 456 Boyle, E, R Collier, AT Dengler, JM Edmond, AC Ng, and RF Stallard. 1974. "On the Chemical  
 457 Mass-Balance in Estuaries." *Geochimica et Cosmochimica Acta* 38 (11): 1719–28.  
 458 [https://doi.org/10.1016/0016-7037\(74\)90188-4](https://doi.org/10.1016/0016-7037(74)90188-4).
- 459 Briant, N, JF Chiffoleau, J Knoery, DF Araújo, E Ponzevera, S Crochet, B Thomas, and C Brach-  
 460 Papa. 2021. "Seasonal Trace Metal Distribution, Partition and Fluxes in the Temperate  
 461 Macrotidal Loire Estuary (France)." *Estuarine, Coastal and Shelf Science* 262 (November):  
 462 107616. <https://doi.org/10.1016/j.ecss.2021.107616>.
- 463 Briant, N, F Elbaz-Poulichet, R Freydier, C Bancon-Montigny, and S Delpoux. 2016. "Deciphering  
 464 As and Cu Cycling in Sediment Pore Waters in a Large Marina (Port Camargue, Southern  
 465 France) Using a Multi-Tracer (Fe, Mn, U, Mo) Approach." *Applied Geochemistry* 66 (March):  
 466 242–49. <https://doi.org/10.1016/j.apgeochem.2016.01.001>.
- 467 Brüggemann, Lutz, Lars Göran Danielsson, Bertil Magnusson, and Stig Westerlund. 1985. "Lead in

- 468 the North Sea and the North East Atlantic Ocean.” *Marine Chemistry* 16 (1): 47–60.  
469 [https://doi.org/10.1016/0304-4203\(85\)90027-1](https://doi.org/10.1016/0304-4203(85)90027-1).
- 470 Cariou, Elsa, Christèle Guivel, Carole La, Laurent Lenta, and Mary Elliot. 2017. “Lead  
471 Accumulation in Oyster Shells, a Potential Tool for Environmental Monitoring.” *Marine*  
472 *Pollution Bulletin* 125 (1–2): 19–29. <https://doi.org/10.1016/J.MARPOLBUL.2017.07.075>.
- 473 Casas, S, JL Gonzalez, B Andral, and D Cossa. 2008. “Relation between Metal Concentration in  
474 Water and Metal Content of Marine Mussels (*Mytilus Galloprovincialis*): Impact of  
475 Physiology.” *Environmental Toxicology and Chemistry / SETAC* 27 (7): 1543–52.  
476 <https://doi.org/10.1897/07-418>.
- 477 Chen, Mengli, Edward A. Boyle, Jong-Mi Lee, Intan Nurhati, Cheryl Zurbrick, Adam D. Switzer,  
478 and Gonzalo Carrasco. 2016. “Lead Isotope Exchange between Dissolved and Fluvial  
479 Particulate Matter: A Laboratory Study from the Johor River Estuary.” *Philosophical*  
480 *Transactions of the Royal Society A: Mathematical, Physical and Engineering Sciences* 374  
481 (2081): 20160054. <https://doi.org/10.1098/rsta.2016.0054>.
- 482 Chételat, John, Brian Cousens, Craig E. Hebert, Thomas S. Jung, Lukas Mundy, Philippe J.  
483 Thomas, and Shuangquan Zhang. 2022. “Isotopic Evidence for Bioaccumulation of Aerosol  
484 Lead in Fish and Wildlife of Western Canada.” *Environmental Pollution* 302 (June): 119074.  
485 <https://doi.org/10.1016/J.ENVPOL.2022.119074>.
- 486 Chouvelon, Tiphaine, Emilie Strady, Mireille Harmelin-Vivien, Olivier Radakovitch, Christophe  
487 Brach-Papa, Sylvette Crochet, Joël Knoery, et al. 2019. “Patterns of Trace Metal  
488 Bioaccumulation and Trophic Transfer in a Phytoplankton-Zooplankton-Small Pelagic Fish  
489 Marine Food Web.” *Marine Pollution Bulletin* 146 (September): 1013–30.  
490 <https://doi.org/10.1016/J.MARPOLBUL.2019.07.047>.
- 491 Claisse, D. 1989. “Chemical Contamination of French Coasts The Results of a Ten Years Mussel  
492 Watch.” *Marine Pollution Bulletin* 20 (10): 523–28. [https://doi.org/10.1016/0025-](https://doi.org/10.1016/0025-326X(89)90141-0)  
493 [326X\(89\)90141-0](https://doi.org/10.1016/0025-326X(89)90141-0).
- 494 Cloquet, C., J. Carignan, G. Libourel, T. Sterckeman, and E. Perdrix. 2006. “Tracing Source  
495 Pollution in Soils Using Cadmium and Lead Isotopes.” *Environmental Science & Technology*  
496 40 (8): 2525–30.
- 497 Couture, R-M, JF Chiffolleau, D Auger, D Claisse, C Gobeil, and D Cossa. 2010. “Seasonal and  
498 Decadal Variations in Lead Sources to Eastern North Atlantic Mussels.” *Environmental*  
499 *Science & Technology* 44 (4): 1211–16. <https://doi.org/10.1021/es902352z>.
- 500 Danielsson, Lars Göran, Bertil Magnusson, Stig Westerlund, and Kerong Zhang. 1982. “Trace  
501 Metal Determinations in Estuarine Waters by Electrothermal Atomic Absorption Spectrometry  
502 after Extraction of Dithiocarbamate Complexes into Freon.” *Analytica Chimica Acta* 144 (C):  
503 183–88. [https://doi.org/10.1016/S0003-2670\(01\)95531-X](https://doi.org/10.1016/S0003-2670(01)95531-X).
- 504 Daskalakis, Kostas D. 1996. “Variability of Metal Concentrations Oyster Tissue and Implications to  
505 Biomonitoring.” *Marine Pollution Bulletin* 32 (11): 794–801. [https://doi.org/10.1016/S0025-](https://doi.org/10.1016/S0025-326X(96)00042-2)  
506 [326X\(96\)00042-2](https://doi.org/10.1016/S0025-326X(96)00042-2).
- 507 Demaure, J.C. 1979. “Les Contraintes Écologiques de l’aménagement de La Loire.” *Penn Ar Bed*  
508 12 (97): 57–72.
- 509 Elbaz-Poulichet, F, P Holliger, WW Huang, and JM Martin. 1984. “Lead Cycling in Estuaries,  
510 Illustrated by the Gironde Estuary, France.” *Nature* 308: 409–14.

- 511 <http://www.nature.com/nature/journal/v308/n5958/abs/308409a0.html>.
- 512 Elbaz-Poulichet, F, P Holliger, JM Martin, and D Petit. 1986. "Stable Lead Isotopes Ratios in Major  
513 French Rivers and Estuaries." *Science of The Total Environment* 54: 61–76.  
514 <http://www.sciencedirect.com/science/article/pii/0048969786902561>.
- 515 Ferrand, J. L., B. Hamelin, and A. Monaco. 1999. "Isotopic Tracing of Anthropogenic Pb  
516 Inventories and Sedimentary Fluxes in the Gulf of Lions (NW Mediterranean Sea)."  
517 *Continental Shelf Research* 19 (1): 23–47.
- 518 Gautier, Emmanuèle, and Stéphane Grivel. 2006. "Multi-Scale Analysis of Island Formation and  
519 Development in the Middle Loire River, France." In *IAHS-AISH Publication*, 306:179–87.  
520 <https://iahs.info/uploads/dms/13547.26-179-187-62-306-Gautier---Grivel.pdf>.
- 521 Goldberg, ED. 1975. "The Mussel Watch-a First Step in Global Marine Monitoring." *Marine*  
522 *Pollution Bulletin* 6: 111. [https://doi.org/10.1016/0025-326X\(75\)90271-4](https://doi.org/10.1016/0025-326X(75)90271-4).
- 523 Harlavan, Y., A. Almogi-Labin, and B. Herut. 2010. "Tracing Natural and Anthropogenic Pb in  
524 Sediments along the Mediterranean Coast of Israel Using Pb Isotopes." *Environmental Science*  
525 *& Technology* 44 (17): 6576–82.
- 526 Hu, Bangqi, Jun Li, Naishuang Bi, Houjie Wang, John Yang, Helong Wei, Jingtao Zhao, et al.  
527 2015. "Seasonal Variability and Flux of Particulate Trace Elements from the Yellow River:  
528 Impacts of the Anthropogenic Flood Event." *Marine Pollution Bulletin* 91 (1): 35–44.  
529 <https://doi.org/10.1016/j.marpolbul.2014.12.030>.
- 530 Komárek, Michael, Vojtěch Ettler, Vladislav Chrastný, and Martin Mihaljevič. 2008. "Lead  
531 Isotopes in Environmental Sciences: A Review." *Environment International*.  
532 <https://doi.org/10.1016/j.envint.2007.10.005>.
- 533 Li, Miling, Dominique Weis, Kate E. Smith, Alyssa E. Shiel, Wade D. Smith, Brian P.V. Hunt, Abe  
534 Torchinsky, and Evgeny A. Pakhomov. 2020. "Assessing Lead Sources in Fishes of the  
535 Northeast Pacific Ocean." *Anthropocene* 29 (March): 100234.  
536 <https://doi.org/10.1016/J.ANCENE.2019.100234>.
- 537 Luoma, Samuel N., and James A. Davis. 1983. "Requirements for Modeling Trace Metal  
538 Partitioning in Oxidized Estuarine Sediments." *Marine Chemistry* 12 (2–3): 159–81.  
539 [https://doi.org/10.1016/0304-4203\(83\)90078-6](https://doi.org/10.1016/0304-4203(83)90078-6).
- 540 Metian, Marc, Michel Warnau, Tiphaine Chauvelon, Fernando Pedraza, Alessia M. Rodriguezy  
541 Baena, and Paco Bustamante. 2013. "Trace Element Bioaccumulation in Reef Fish from New  
542 Caledonia: Influence of Trophic Groups and Risk Assessment for Consumers." *Marine*  
543 *Environmental Research* 87–88 (June): 26–36.  
544 <https://doi.org/10.1016/J.MARENRES.2013.03.001>.
- 545 Monna, F., K. Hamer, J. Lévêque, and M. Sauer. 2000. "Pb Isotopes as a Reliable Marker of Early  
546 Mining and Smelting in the Northern Harz Province (Lower Saxony, Germany)." *Journal of*  
547 *Geochemical Exploration* 68 (3): 201–10. [https://doi.org/10.1016/S0375-6742\(00\)00005-4](https://doi.org/10.1016/S0375-6742(00)00005-4).
- 548 Monna, F, J Lancelot, I Croudace, A Cundy, and JT Lewis. 1997. "Pb Isotopic Composition of  
549 Airborne Particulate Material from France and the Southern United Kingdom : Implications for  
550 Pb Pollution Sources in Urban Areas Pb Isotopic Composition of Airborne Particulate Material  
551 from France and the Southern United Kingdo." *Environmental Science & Technology* 31 (8):  
552 2277–86. <https://doi.org/10.1021/es960870>.
- 553 Négrel, Philippe, and Emmanuelle Petelet-Giraud. 2012. "Isotopic Evidence of Lead Sources in

- 554 Loire River Sediment.” *Applied Geochemistry* 27 (10): 2019–30.  
555 <https://doi.org/10.1016/j.apgeochem.2012.05.015>.
- 556 Ottmann, F. 1979. “Conséquences Des Aménagements Sur Le Milieu Estaurien.” *Journal de*  
557 *Recherche En Océanographie* 4 (2): 11–24.
- 558 Rabinowitz, Michael B., and George W. Wetherill. 1972. “Identifying Sources of Lead  
559 Contamination by Stable Isotope Techniques.” *Environmental Science and Technology* 6 (8):  
560 705–9. <https://doi.org/10.1021/es60067a003>.
- 561 Saulnier, I, and A Mucci. 2000. “Trace Metal Remobilization Following the Resuspension of  
562 Estuarine Sediments: Saguenay Fjord, Canada.” *Applied Geochemistry* 15 (2): 191–210.  
563 [https://doi.org/10.1016/S0883-2927\(99\)00034-7](https://doi.org/10.1016/S0883-2927(99)00034-7).
- 564 Shiel, AE, D Weis, and KJ Orians. 2012. “Tracing Cadmium, Zinc and Lead Sources in Bivalves  
565 from the Coasts of Western Canada and the USA Using Isotopes.” *Geochimica et*  
566 *Cosmochimica Acta* 76: 175–90.  
567 <http://www.sciencedirect.com/science/article/pii/S0016703711005928>.
- 568 Shoty, W, D Weiss, PG Appleby, AK Cheburkin, R Frei, JD Kramers, S Reese, and WO Van der  
569 Knaap. 1998. “History of Atmospheric Lead Deposition Since 12,370 14C Yr BP from a Peat  
570 Bog, Jura Mountains, Switzerland.” *Science* 281 (5383): 1635–40.  
571 <https://doi.org/10.1126/science.281.5383.1635>.
- 572 Souza Machado, Anderson Abel de, Kate Spencer, Werner Kloas, Marco Toffolon, and Christiane  
573 Zarfl. 2016. “Metal Fate and Effects in Estuaries: A Review and Conceptual Model for Better  
574 Understanding of Toxicity.” *Science of The Total Environment* 541 (January): 268–81.  
575 <https://doi.org/10.1016/J.SCITOTENV.2015.09.045>.
- 576 Sung, W. 1995. “Some Observations on Surface Partitioning of Cd, Cu, and Zn in Estuaries.”  
577 *Environmental Science & Technology* 29 (5): 1303–12.
- 578 Thévenot, D, L Lestel, MH Tusseau-Vuillemin, JL Gonzales, and M Meybeck. 2009. “Les Métaux  
579 Dans Le Bassin de La Seine - Comprendre d’où Proviennent et Comment Circulent Les  
580 Métaux Dans Un Bassin Versant Fortement Exposé Aux Pressions Humaines.” *Collection Du*  
581 *Programme PIREN-Seine*, 60.
- 582 Waeles, M, R Riso, JF Maguer, JF Guillaud, and P Le Corre. 2008. “On the Distribution of  
583 Dissolved Lead in the Loire Estuary and the North Biscay Continental Shelf, France.” *Journal*  
584 *of Marine Systems* 72 (1–4): 358–65. <https://doi.org/10.1016/j.jmarsys.2007.01.012>.
- 585 Wiederhold, Jan G. 2015. “Metal Stable Isotope Signatures as Tracers in Environmental  
586 Geochemistry.” *Environmental Science and Technology*. <https://doi.org/10.1021/es504683e>.
- 587 Windom, H, and F Niencheski. 2003. “Biogeochemical Processes in a Freshwater–Seawater Mixing  
588 Zone in Permeable Sediments along the Coast of Southern Brazil.” *Marine Chemistry* 83 (3–  
589 4): 121–30. [https://doi.org/10.1016/S0304-4203\(03\)00106-3](https://doi.org/10.1016/S0304-4203(03)00106-3).

590

591

Table I: Metadata, chemical characteristics, Pb concentrations and isotope ratios of water and suspended particulate material at the sampled stations for the three CAMELIA campaigns.  $Q_{\text{Loire River}} \sim 210 \text{ m}^3 \text{ s}^{-1}$  with rising tide during the 2012 campaign,  $Q_{\text{Loire River}} \sim 1673 \text{ m}^3 \text{ s}^{-1}$  with rising tide during the 2013 campaign and  $Q_{\text{Loire River}} \sim 2790 \text{ m}^3 \text{ s}^{-1}$  with ebb tide during the 2014 campaign. (SPM: suspended particulate material; Pbd : dissolved Pb, Pbp : particulate Pb, n.d : not-determined)

N° station	Latitude	Longitude	date	salinity	SPM ( $\text{mg L}^{-1}$ )	Pbd (nM)	Pbp ( $\text{mg kg}^{-1}$ )	log Kd	$^{206}/^{207}\text{Pbd}$	$^{206}/^{208}\text{Pbd}$	$^{206}/^{207}\text{Pbp}$	$^{206}/^{208}\text{Pbp}$
<b>Montjean (River site)</b>	47.3929	-0.8607	19/09/2012	0.0	14.4	0.09	45.7	6.4	1.172	0.479	1.182	0.480
<b>Tabarly bridge</b>	47.2121	-1.5289	19/09/2012	0.0	269.7	0.11	60.8	6.4	1.165	0.476	1.176	0.479
<b>CAM1 ST15</b>	47.2699	-2.1885	28/09/2012	23.7	83.1	0.26	70.5	6.1	1.161	0.476	1.174	0.479
<b>CAM1 ST16</b>	47.2872	-2.1673	28/09/2012	22.9	39.7	0.14	58.1	6.3	1.161	0.477	1.175	0.480
<b>CAM1 ST17</b>	47.3007	-2.1235	28/09/2012	17.2	71.1	0.15	55	6.3	1.167	0.477	1.177	0.480
<b>CAM1 ST18</b>	47.3034	-2.1007	28/09/2012	14.2	212.9	0.15	64.1	6.3	1.162	0.476	1.178	0.479
<b>CAM1 ST19</b>	47.3007	-2.0502	28/09/2012	11.2	1413.2	0.14	67.1	6.4	1.162	0.476	1.180	0.481
<b>CAM1 ST20</b>	47.2937	-2.0202	28/09/2012	8.2	1146.3	0.19	72.6	6.3	1.166	0.478	1.176	0.479
<b>CAM1 ST21</b>	47.2909	-2.0127	28/09/2012	5.4	2106.2	0.15	77.9	6.4	1.165	0.477	1.174	0.480
<b>CAM1 ST22</b>	47.2875	-1.9966	28/09/2012	3.2	1323.8	0.14	76.1	6.4	1.164	0.477	1.175	0.479
<b>CAM1 ST23</b>	47.2842	-1.9725	28/09/2012	1.6	751.2	0.14	67.2	6.3	1.161	0.477	1.174	0.480
<b>CAM1 ST24</b>	47.2811	-1.9261	28/09/2012	0.0	999.6	0.13	72.9	6.4	1.164	0.475	1.178	0.480
<b>Montjean (River site)</b>	47.3929	-0.8607	15/04/2013	0.0	60.8	0.14	55.7	6.3	n.d	n.d	n.d	n.d
<b>Tabarly bridge</b>	47.2121	-1.5289	15/04/2013	0.0	64.9	0.15	58	6.3	n.d	n.d	n.d	n.d
<b>CAM-2 ST12</b>	47.1530	-2.3278	25/04/2013	27.5	9.4	0.04	61.5	6.8	n.d	n.d	n.d	n.d
<b>CAM-2 ST13</b>	47.1721	-2.3065	25/04/2013	22.1	27.4	0.06	51.3	6.6	n.d	n.d	n.d	n.d
<b>CAM-2 ST14</b>	47.1950	-2.2896	25/04/2013	22.0	21.9	0.10	60.8	6.5	n.d	n.d	n.d	n.d
<b>CAM-2 ST15</b>	47.2109	-2.2800	25/04/2013	17.7	45.0	0.09	61.4	6.5	n.d	n.d	n.d	n.d
<b>CAM-2 ST16</b>	47.2161	-2.2763	25/04/2013	16.2	66.1	0.10	64.8	6.5	n.d	n.d	n.d	n.d

<b>CAM-2 ST17</b>	47.2782	-2.1784	26/04/2013	13.2	74.7	0.06	64	6.7	n.d	n.d	n.d	n.d
<b>CAM-2 ST18</b>	47.2878	-2.1658	26/04/2013	10.3	43.8	0.07	55.1	6.6	n.d	n.d	n.d	n.d
<b>CAM-2 ST19</b>	47.2994	-2.1375	26/04/2013	7.1	97.7	0.07	65.2	6.7	n.d	n.d	n.d	n.d
<b>CAM-2 ST20</b>	47.3040	-2.1051	26/04/2013	4.1	91.3	0.07	63.8	6.6	n.d	n.d	n.d	n.d
<b>CAM-2 ST21</b>	47.3025	-2.0689	26/04/2013	1.0	411.2	0.15	71.3	6.4	n.d	n.d	n.d	n.d
<b>CAM-2 ST22</b>	47.1997	-1.6842	26/04/2013	0.0	21.7	0.09	48	6.4	n.d	n.d	n.d	n.d
<b>Montjean (River site)</b>	47.3929	-0.8607	28/01/2014	0.0	52.6	0.16	64.9	6.3	n.d	n.d	n.d	n.d
<b>Tabarly bridge</b>	47.2121	-1.5289	28/01/2014	0.0	58.5	0.15	59.2	6.3	n.d	n.d	n.d	n.d
<b>CAM-3 ST1</b>	47.1969	-1.5819	01/02/2014	0.0	46.1	0.18	51.3	6.1	n.d	n.d	n.d	n.d
<b>CAM-3 ST2</b>	47.1986	-1.6812	01/02/2014	0.0	60.1	0.14	55.7	6.3	n.d	n.d	n.d	n.d
<b>CAM-3 ST3</b>	47.2992	-2.1373	01/02/2014	0.0	381.1	n.d	64	5.5	n.d	n.d	n.d	n.d
<b>CAM-3 ST4</b>	47.298	-2.1413	01/02/2014	0.1	683.7	0.16	67.9	6.3	n.d	n.d	n.d	n.d
<b>CAM-3 ST5</b>	47.2972	-2.1451	01/02/2014	3.7	493.0	0.20	68.1	6.2	n.d	n.d	n.d	n.d
<b>CAM-3 ST6</b>	47.2843	-2.1707	01/02/2014	6.4	144.1	0.12	61.7	6.4	n.d	n.d	n.d	n.d
<b>CAM-3 ST7</b>	47.2677	-2.1906	01/02/2014	8.9	95.9	0.10	62.3	6.5	n.d	n.d	n.d	n.d
<b>CAM-3 ST8</b>	47.236	-2.2545	02/02/2014	11.2	51.3	0.09	57.6	6.5	n.d	n.d	n.d	n.d
<b>CAM-3 ST9</b>	47.1769	-2.3037	02/02/2014	13.7	66.7	0.09	57.2	6.5	n.d	n.d	n.d	n.d
<b>CAM-3 ST10</b>	47.1729	-2.3062	02/02/2014	17.1	40.3	0.09	55.2	6.5	n.d	n.d	n.d	n.d
<b>CAM-3 ST11</b>	47.1651	-2.3124	02/02/2014	20.2	26.4	0.08	58.4	6.5	n.d	n.d	n.d	n.d
<b>CAM-3 ST12</b>	47.1354	-2.3538	02/02/2014	21.9	22.8	0.08	53.7	6.5	n.d	n.d	n.d	n.d
<b>CAM-3 ST13</b>	47.1263	-2.3673	02/02/2014	24.0	21.9	0.06	55.6	6.7	n.d	n.d	n.d	n.d



Table II: Lead concentrations and isotope composition of sediment samples (surface sediments and PV1 sediment core). EF: Enrichment Factor from the local geochemical background (LB).

Number in Fig. 1	Site	Pb (mg kg <sup>-1</sup> )	Al (%)	Pb Normalized	EF <sub>LB</sub>	<sup>206</sup> / <sub>207</sub> Pb	<sup>206</sup> / <sub>208</sub> Pb
1	Ste Luce – 44 L014	63.6	6.2	10.3	1.0	1.175	0.479
2	Indre - 44 L015	64.3	6.2	10.4	1.0	1.180	0.480
3	Paimboeuf	88.5	7.3	12.1	1.1	1.158	0.473
4	Pont de Saint-Nazaire amont	45.1	4.9	9.2	0.9	1.169	0.477
5	Face pointe de Mindin	65.7	6.8	9.6	0.9	1.176	0.480
6	St Brévin Mindin	63.4	7.4	8.6	0.8	1.179	0.479
7	Villes - Martin (a)	38.0	4.6	8.3	0.8	1.172	0.477
8	Face St Brévin	53.9	6.2	8.8	0.8	1.182	0.478
9	Est Petit Gavi	53.8	6.3	8.6	0.8	1.181	0.479
10	Ouest Lancastria	40.3	5.2	7.8	0.7	1.175	0.478
11	Sud phare de la Banche	57.9	6.4	9.0	0.8	1.177	0.479
12	Loire 26	55.5	6.8	8.2	0.8	1.178	0.479
13	Banc de Bourgneuf	48.2	5.5	8.7	0.8	1.177	0.477
14	Coupelasse Nord	30.6	4.7	6.5	0.6	1.178	0.479
15	Mariolle HF3	15.8	6.8	2.3	0.2	1.187	0.480
16	Noirmoutier – Gresse-loup	34.3	3.0	11.4	1.1	1.179	0.479
17	Embarcadère	23.9	2.0	11.9	1.1	1.183	0.480
<i>PV1 sediment core</i>							
	1 cm	88.5	7.3			1.158	0.473
	6 cm	90.9	7.0			1.156	0.474
	9 cm	103.5	7.1			1.150	0.473
	14 cm	134.1	7.6			1.142	0.472
	21 cm	131.5	7.6			1.146	0.472
	35 cm	124.4	7.4			1.161	0.476
	42 cm	105.9	7.4			1.162	0.476
	69 cm	116.2	7.4			1.158	0.475
	96 cm	75.8	6.4			1.179	0.479
	163 cm	83.2	6.8			1.178	0.478
	210 cm	75.4	6.6			1.179	0.479
	296 cm	58.1	6.1			1.184	0.479
	390 cm	101.8	6.8			1.182	0.480
	495 cm	107.6	6.8			1.183	0.481

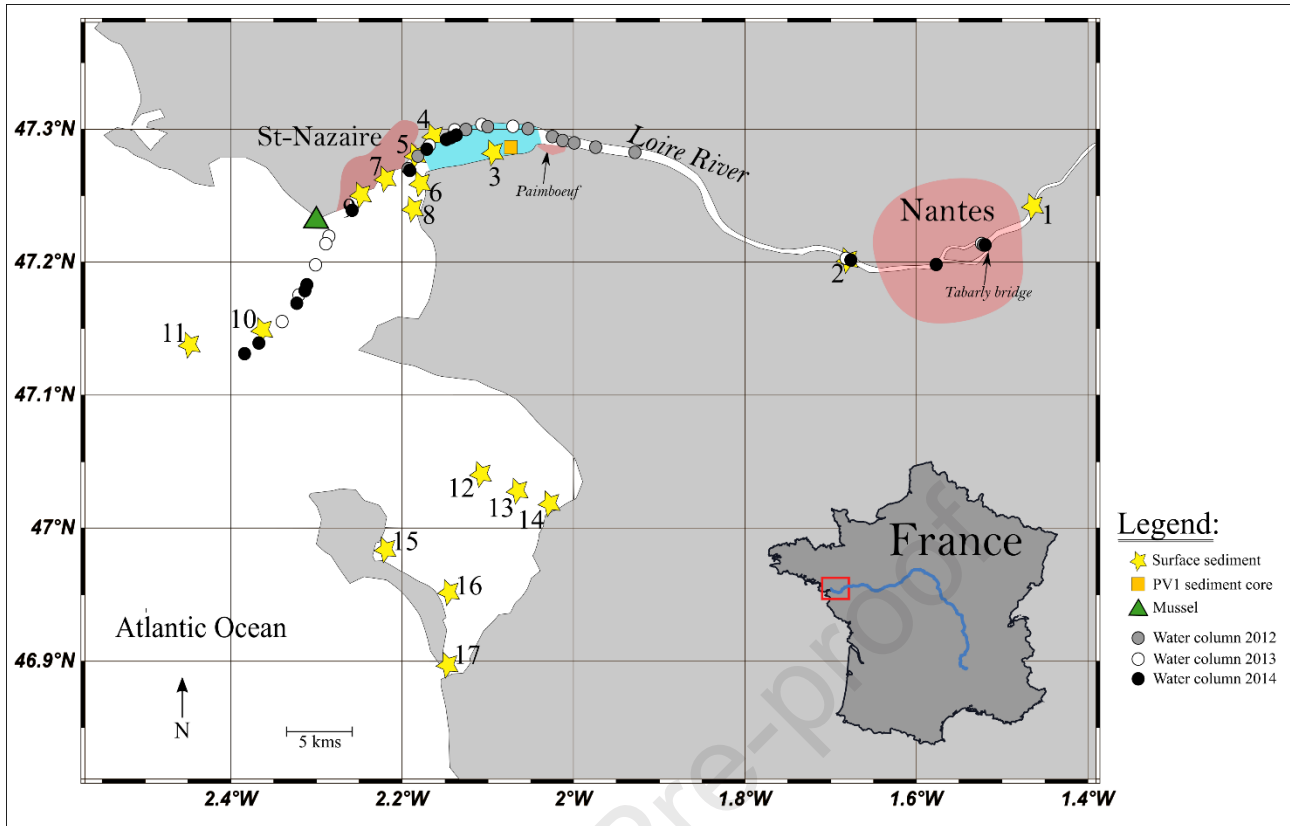


Figure 1: Sampling sites in the Loire estuary. Circles are water sampling sites during the CAMELIA campaigns in September 2012 (gray). April 2013 (white) and February 2014 (black). Yellow stars and the orange square are sediment sampling sites numbered in Table 1. The green triangle is the location of the bed of wild mussels (*Mytilus edulis*) “Pointe Chemoulin” of the ROCCh monitoring program. Shrimps and seabass sampling area is represented by the light blue area. The light red areas correspond to the main cities along the estuary.

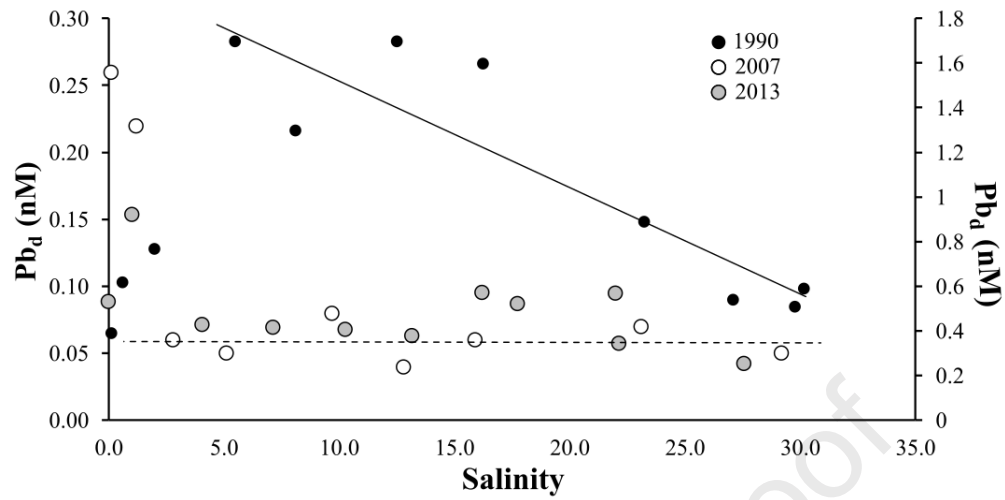


Figure 2: Comparison of Pb<sub>d</sub> concentrations along the Loire Estuary salinity gradient for the three Loire estuary studies. Black dots are data from Boutier et al., 1990 with the right y-axis. White dots are data from Waeles et al., 2007 study and grey dots correspond to this study. Solid line: best fit for salinity range 5-30 (Boutier et al., 1990) used in the 1990 flux computation.

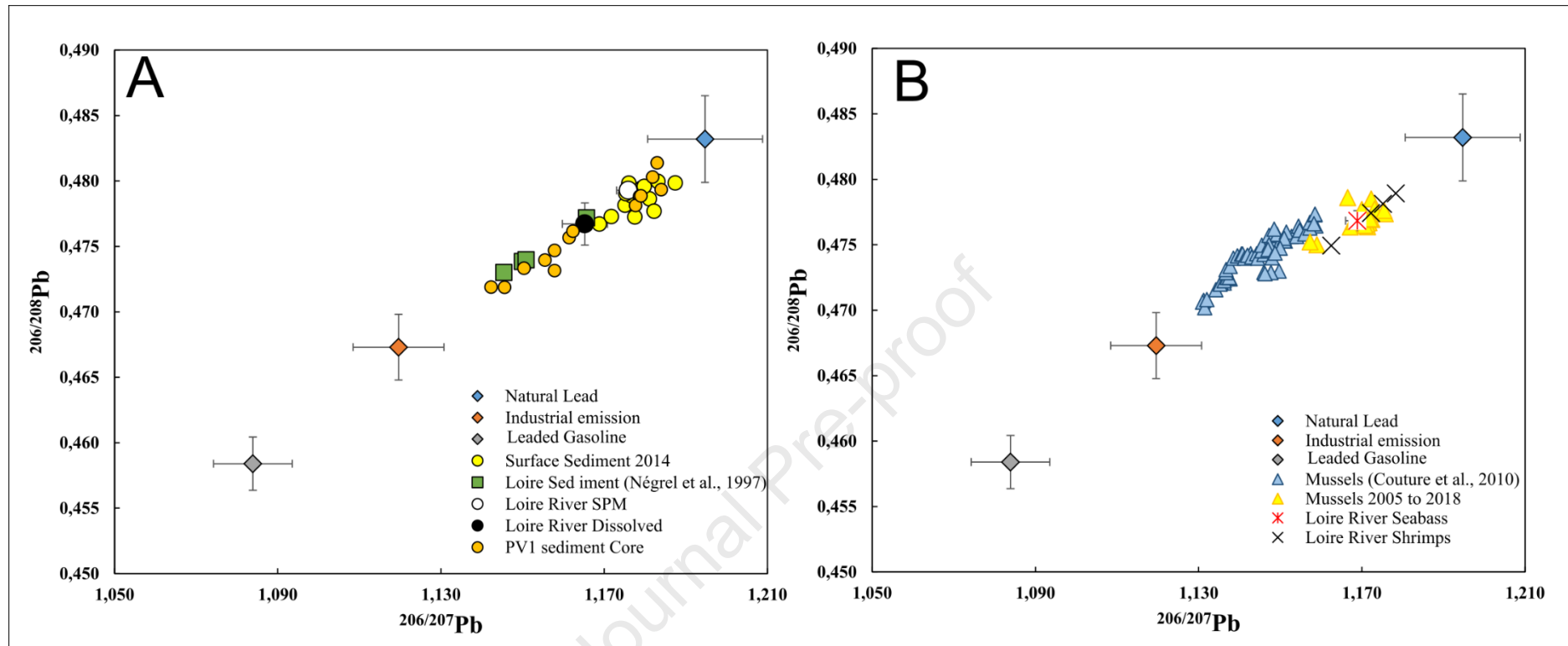


Figure 3: Isotope Pb ratios distribution in Loire River water column and sediments (A). Lead gasoline and industrial emissions correspond to data from Monna et al.. (1997). Natural lead corresponds to background values from Komárek et al.. (2008). Isotope Pb ratios distribution in biological tissue from Loire River fauna (B).

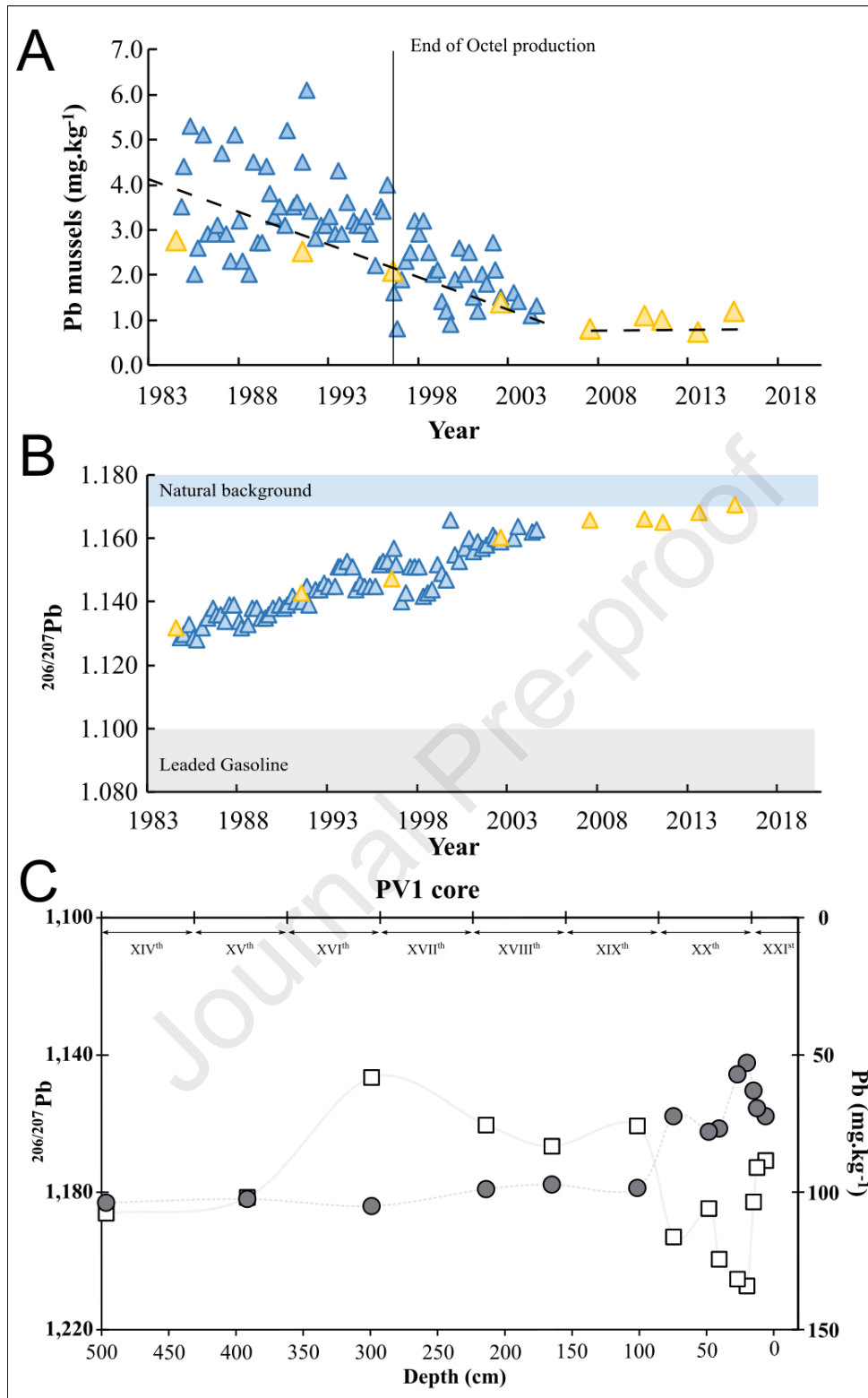


Figure 4: Mussels Pb concentrations (A) and <sup>206/207</sup>Pb isotopes ratios (B). Blue triangles are data from Couture et al., 2010 and yellow triangles are from this study. Sediment core Pb concentrations and <sup>206/207</sup>Pb isotopes ratios (C). Roman numbers represent the estimated centuries.

## Authors contributions

**Nicolas Briant:** Data interpretation, Writing- Original draft preparation, Reviewing and Editing. **Joël Knoery** and **Christophe Brach-Papa:** Conceptualization, Methodology, Reviewing, Supervision. **Sandrine Bruzac, Teddy Sireau** and **Bastien Thomas:** Methodology, Analytics and data generation. **Tiphaine Chauvelon, Emmanuel Ponzevera** and **Daniel F. Araujo:** Writing- Reviewing. **Edouard Metzger** and **Meryem Mojtahid:** Conceptualization of the cruise, Reviewing. All authors commented on the manuscript. All authors read and approved the revised manuscript

**Declaration of interests**

The authors declare that they have no known competing financial interests or personal relationships that could have appeared to influence the work reported in this paper.

The authors declare the following financial interests/personal relationships which may be considered as potential competing interests:

Journal Pre-proof